Supramolecular Assemblies of Histidinylated α-Cyclodextrin in the Presence of DNA Scaffold during CDplexes Formation

ARTICLE *in* BIOCONJUGATE CHEMISTRY · DECEMBER 2011

Impact Factor: 4.51 · DOI: 10.1021/bc200167p · Source: PubMed

6 AUTHORS, INCLUDING:

Véronique Bennevault-Celton
Université d'Évry-Val-d'Essonne
25 PUBLICATIONS **196** CITATIONS
SEE PROFILE

Olivier Martin
Université d'Orléans
148 PUBLICATIONS **2,760** CITATIONS
SEE PROFILE

Chantal Pichon
CNRS Orleans Campus and University of Orl…
146 PUBLICATIONS **2,453** CITATIONS
SEE PROFILE

Patrick Midoux
CNRS Orleans Campus
168 PUBLICATIONS **5,086** CITATIONS
SEE PROFILE

Bioconjugate Chemistry

Article

pubs.acs.org/bc

Supramolecular Assemblies of Histidinylated α-Cyclodextrin in the Presence of DNA Scaffold during CDplexes Formation

Véronique Bennevault-Celton,[#,‡] Allan Urbach,[#,§] Olivier Martin,[§] Chantal Pichon,[†] Philippe Guégan,[‡] and Patrick Midoux*[,†]

[†]Centre de Biophysique Moléculaire CNRS UPR 4301, University of Orléans and Inserm, Rue Charles Sadron, F-45071 Orléans Cedex 2, France

[‡]Laboratoire Analyse et Modélisation pour la Biologie et l'Environnement, CNRS UMR8587, University of Evry Val d'Essonne, Rue du Père Jarlan, 91025 Evry Cedex, France

[§]Institut de Chimie Organique et Analytique, UMR CNRS 6005, University of Orléans, 45067 Orléans cedex 2, France

Supporting Information

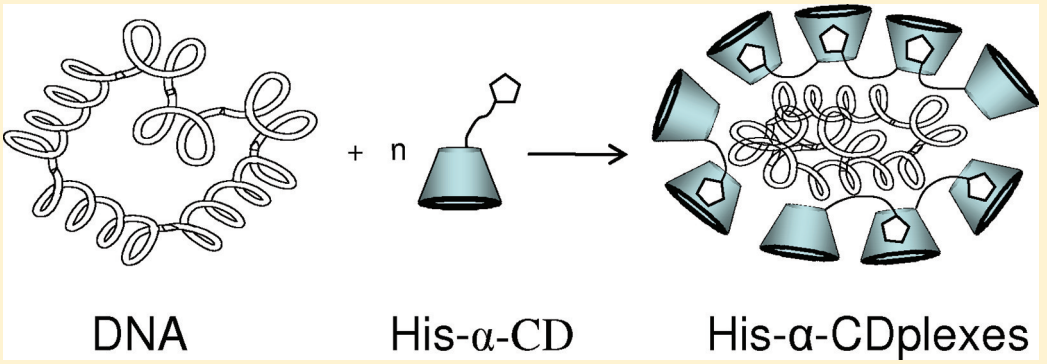

ABSTRACT: α-Cyclodextrin was transformed in a cationic unit after *per* substitution with histidine (His-α-CD) and lysine (Lys-α-CD) molecules on the primary face. His-α-CD and Lys-α-CD were used to form electrostatic complexes (CDplexes) with a plasmid DNA encoding luciferase gene, and the ability of CDplexes to transfect mammalian cells was examined using HEK293-T7 cells. The luciferase activity in cells transfected with His-α-CDplexes was 8-fold higher than that obtained Lys-α-CDplexes. When the transfection was carried out in the presence of chloroquine, the luciferase activity with His-α-CDplexes and Lys-α-CDplexes increased 6 and 25 times, respectively. The lower enhancement with His-α-CDplexes confirmed that histidine induced a proton sponge effect inside endosomes upon imidazole protonation, favoring DNA delivery in the cytosol. At the same time, we found that the condensation of DNA with His-α-CD was unexpectedly stronger than that obtained with the lysyl-α-CD counterpart. Moreover, it was as strong as that observed with high molecular weight polylysine. NMR (ROESY and DOSY) investigations in the absence of DNA showed that an inclusion complex is formed between the imidazole ring of histidine and the hydrophobic cavity of CD but no His-α-CD polymers can be formed by intermolecular interactions. These results suggest that intermolecular interactions between imidazole and His-α-CD cavity could be involved to form supramolecular assemblies in the presence of a DNA scaffold leading to DNA condensation into low diameter particles.

INTRODUCTION

Cyclodextrins are natural biocompatible cyclic oligosaccharides composed of 6, 7, or 8 D(+)-glucose units linked by α-1,4-linkages and named α-, β-, or γ-cyclodextrin, respectively. Recently, various cyclodextrin-based gene delivery systems have been developed.[1] For instance, cyclodextrin can be transformed in a cationic unit after *per* substitution with small cationic molecules. These derivatives can condense a plasmid DNA (pDNA) to form CDplexes that can be used for the transfection of mammalian cells. For example, α- and β-cyclodextrins have been *per* substituted with oligoethylenimine repeat units (from 1 to 14).[2,3] The transfection efficiency of HEK293 and COS-7 cells increased as the length of the oligoethylenimine moiety increased from diethylenetriamine to pentaethylenehexamine residues. β-Cyclodextrin was used also as a scaffold to prepare a homogeneous sevenfold symmetric polyaminothiourea amphiphiles for gene transfer.[4−6] Cationic cyclodextrins have been derivatived in cationic polyrotaxanes either with a poly(ethylene oxide)-poly(propylene oxide)-poly(ethylene oxide) triblock copolymer, a PEI-b-PEG-b-PEI copolymer or α,ω-dimethacrylate poly(ethylene glycol).[7−9] For certain CD derivatives, the transfection efficiency was comparable to that obtained with JetPEI, the gold standard cationic polymer. One of the major barriers for gene transfer is

Received: March 31, 2011
Revised: October 17, 2011
Published: October 21, 2011

Scheme 1. Synthetic Scheme of α-Cyclodextrin Derivatives: (1) NH_2-α-CD; (2) His-α-CD; (3) Lys-α-CD

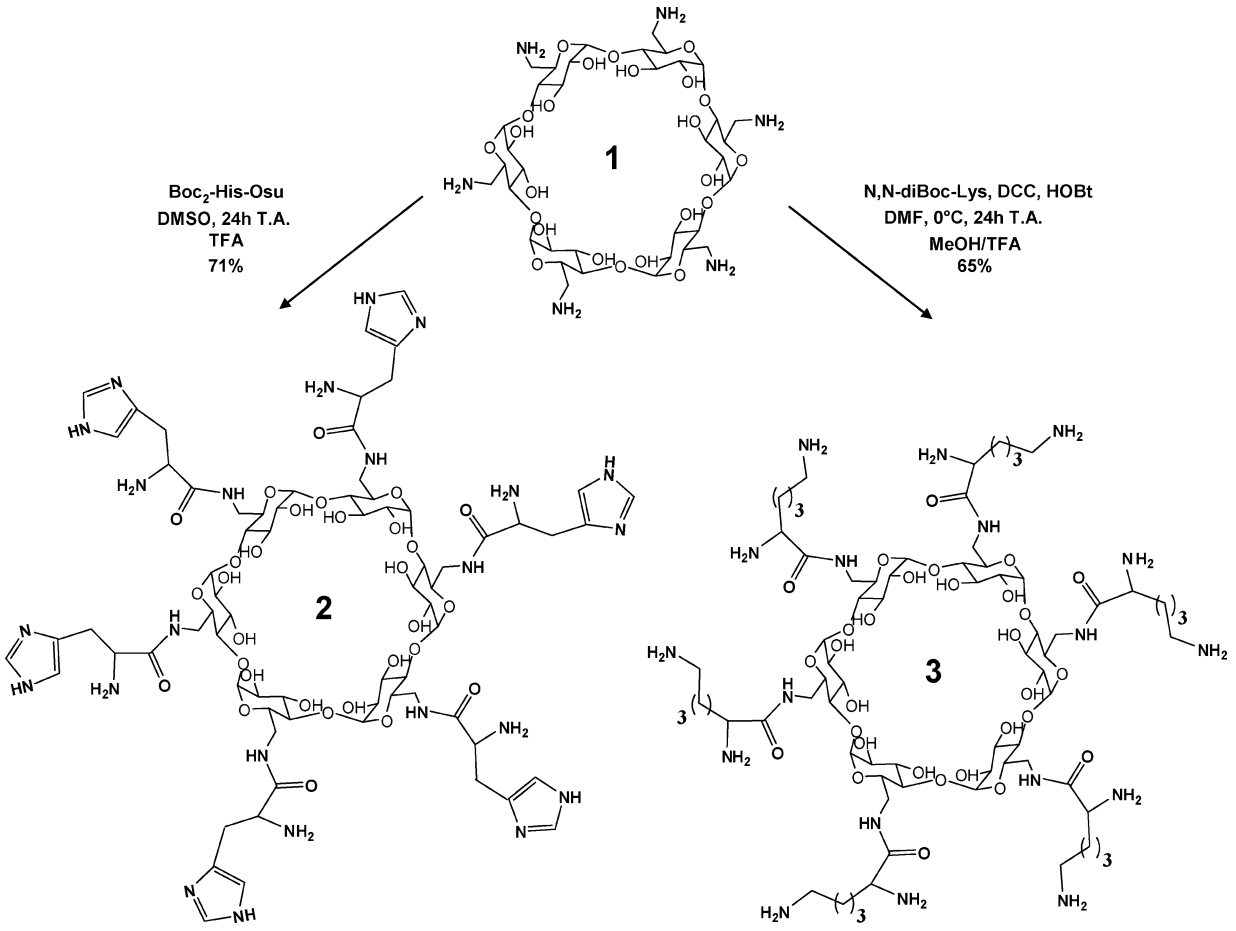

the endosome escape allowing the delivery of the plasmid DNA in the cytosol. For this purpose, histidine can be used. The imidazole ring of histidine is a weak base that has the ability to acquire a cationic charge when the pH of the environment drops below 6. As has been demonstrated for poly(histidine), this phenomenon can induce membrane fusion and/or membrane permeation in an acidic medium.[10,11] Moreover, the accumulation of protonated histidine residues inside acidic vesicles can induce a proton sponge effect, which increases their osmolarity and their swelling. The proof of concept has been shown with polylysine partially substituted with histidine residues that has caused a tremendous increase by 3−4.5 orders of magnitude of the transfection efficiency of DNA/polylysine polyplexes.[12] Then, several histidine-rich polymers and peptides as well as lipids with imidazole polar heads have been reported to be efficient carriers to deliver nucleic acids including DNA and RNA *in vitro* and *in vivo*.[13] More remarkable, histidylated carriers are often weakly cytotoxic, making them promising chemical vectors for nucleic acid delivery.

Here, we have used α-CD as a scaffold to prepare histidylated CD as DNA carrier. α-CD was chosen because of its lower propensity to form an inclusion complex with cholesterol than β-CD.[14−16] Indeed, β-CD has been shown to extract cholesterol from cell membranes. We have synthesized the hexakis(6-deoxy-6-histidinyl)cyclomaltohexaose (His-α-CD) (**2**) (Scheme 1). This derivative had six α-amino groups usable for pDNA interaction and six imidazole rings for acid-mediated membrane destabilization after CDplex uptake by the cells into endosomes. The polyamino α-CD counterparts, the hexakis(6-deoxy-6-amino)cyclomaltohexaose (NH_2-α-CD) (**1**) and the hexakis(6-deoxy-6-lysinyl)cyclomaltohexaose (Lys-α-CD) (**3**), were also synthesized (Scheme 1). The former had six amino groups as His-α-CD and the latter twelve. The capacity of these cationic α-CD derivatives to condense pDNA was determined and the transfection efficiency of CDplexes was evaluated in HEK293-T7 cells using the luciferase gene as read-out. Unexpectedly, a strong condensation of pDNA by His-α-CD was evidenced. Furthermore, we showed by NMR investigations the involvement of an inclusion complex between the imidazole ring of histidine and the hydrophobic cavity of CD. These results suggest that supramolecular assemblies of His-α-CD in the presence of a DNA scaffold could occur during the formation of His-α-CDplexes.

EXPERIMENTAL PROCEDURES

All reagents were purchased from Sigma (St. Quentin Fallavier, France) unless otherwise stated.

The synthesis of hexakis(6-deoxy-6-iodo)cyclomaltohexaose has been adapted from ref 17, and hexakis(6-deoxy-6-azido)cyclomaltohexaose from ref 3 and hexakis(6-deoxy-6-amino)cyclomaltohexaose from ref 18. The detailed experimental protocols and the characterizations are reported in the Supporting Information (S1).

Hexakis(6-deoxy-6-histidinyl)cyclomaltohexaose (His-α-CD). Boc_2-His-OSu (0.59 g, 1.30 mmol) was added to a stirring solution of hexakis(6-deoxy-6-amino)-cyclomaltohexaose (0.20 g, 0.207 mmol) in DMSO (5 mL),

dx.doi.org/10.1021/bc200167p | *Bioconjugate Chem.* 2011, 22, 2404−2414

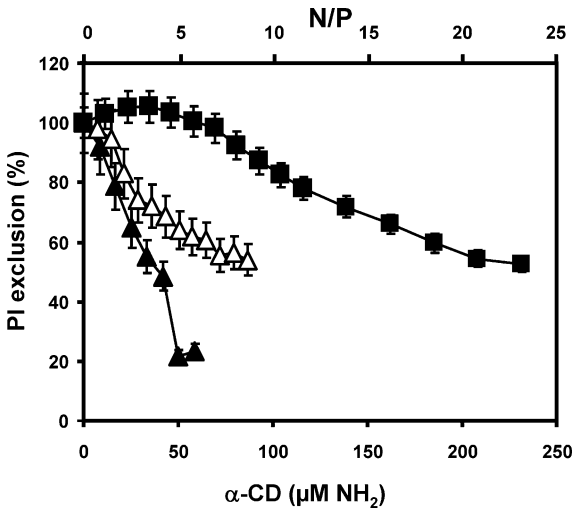

Figure 1. Interaction of polyamino-α-CD derivatives with DNA. Aliquots of solution containing polyamino-α-CD derivatives were sequentially added to pDNA (2.5 μg) in 650 μL of 10 mM Hepes buffer, pH 7.4, in the presence of ethidium bromide (2 μM). The fluorescence intensity was measured (λ_{ex} = 530 nm; λ_{em} = 580 nm) after each addition of samples, and the fraction of dye exclusion was calculated from the fluorescence intensity measured in the absence and in the presence of polyamino-α-CD derivatives. N/P corresponds to the ratio between the number of positive charges of polyamino-α-CD derivatives and that of the negative charges of the pDNA phosphate. His-α-CD (▲); Lys-α-CD (△); NH_2-α-CD (■).

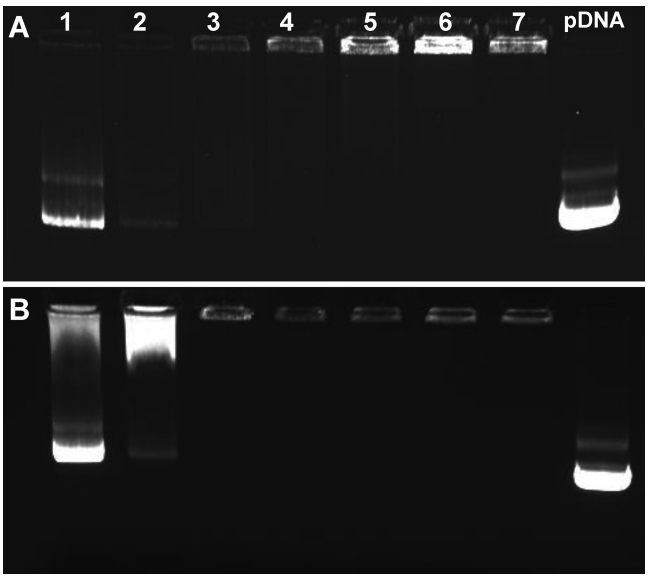

Figure 2. Agarose gel electrophoresis shift assay of pDNA in the presence of various quantities of His-α-CD (A) and Lys-α-CD (B). Lanes 1, 2, 3, 4, 5, 6, 7, and 8 correspond to pDNA/CD weight ratios (μg/μg) of 1/0.5, 1/1, 1/2, 1/3, 1/4, 1/6, and 1/8, respectively. pDNA line correspond to migration of pDNA in the absence of any polyamino α-CD derivatives. Electrophoresis was conducted for 1 h under 80 V/cm through a 0.6% agarose gel containing ethidium bromide (1 μg/mL) in 95 mM Tris, 89 mM boric acid, and 2.5 mM EDTA (pH 8.6). An ultraviolet lightbox was used to visualize ethidium bromide-stained DNA in gels.

and the reaction was carried out at room temperature for 24 h. Then, 2 mL of trifluoroacetic acid (TFA) was added and the medium was stirred for 12 h. After removal of TFA under reduced pressure, the product was recovered by precipitation in ethyl acetate (AcOEt) with 71% yield (0.45 g). ^{1}H NMR (D_2O, 300 MHz): δ ppm 7.7 (H10), 6.9 (H9), 4.5 (H1), 4.0 (H7), 3.8 (H3), 3.6 (H5), 3.5 (H6), 3.3 (H2), 3.0 (H8), 2.8 (H4). ^{13}C NMR (D_2O, 100 MHz): δ ppm 171.7 (C═O, amide), 163.3 (q, C═O, TFA), 136.8 (C-10 arom. imidazole), 132.9 (C quat. arom. imidazole), 116.7 (C-9 arom. imidazole), 117.0 (CF_3, TFA), 101.9 (C-1), 82.6 (C-4), 72.8, 72.1, 69.7 (C-2, C-3, C-5), 53.8 (C-7; $CHNH_3$), 39.6 (C-6), 30.2 (C-8). For $C_{72}H_{108}N_{24}O_{30}$, MS (MALDI-TOF/TOF): 1795.8 uma $[M + Li]^+$, 1827.8 uma $[M + K]^+$.

Hexakis(6-deoxy-6-lysinyl)cyclomaltohexaose (Lys-α-CD). *N*,*N*-diBoc-lysine (0.432 g, 1.24 mmol) was dissolved in dry DMF (10 mL). 1-Hydroxybenzotriazole (HOBt) (0.176 g, 1.30 mmol) was added, and the solution was cooled to 0 °C in an ice bath. *N*,*N*′-Dicyclohexylcarbodiimide (DCC) (0.261 g, 1.27 mmol) was then added, and the temperature was maintained at 0 °C for a further 60 min. The reaction mixture was then allowed to warm to room temperature during which time dicyclohexylurea precipitated out. After stirring for a further 60 min at room temperature, a suspension of hexakis(6-deoxy-6-amino)cyclomaltohexaose (0.200 g, 0.207 mmol) and methyl morpholine (0.14 mL) in dry DMF (5 mL) was added to the reaction medium and the solution was stirred at room temperature for 24 h. The dicyclohexylurea precipitate was filtered off, and the filtrate was concentrated under reduced pressure at 50 °C as oil. Then, saturated $NaHCO_3$ (100 mL) was added to the oil to give a suspension which was stirred for 1 h and filtered. The precipitate was washed with H_2O and dried under high vacuum. The crude product underwent subsequent Boc deprotection in a MeOH/TFA (10:2; v/v) solution at room temperature, and the solvent was evaporated and replaced by AcOEt (5 mL). The precipitate was filtered and the expected product was recovered in 65% yield (0.418 g). ^{1}H NMR (D_2O, 500 MHz): δ ppm 4.95 (d, 6 H), 3.40−4.08 (m, 36 H), 3.31 (m, 6 H), 3.02 (m, 12 H), 1.96 (m, 12 H), 1.74 (m, 12 H), 1.49 (m, 12 H). ^{13}C NMR (D_2O, 125 MHz): δ ppm 170.1 (C═O, amide), 162.6−163.4 (C═O, TFA), 113.1−120.1 (CF_3), 102.1 (C-1), 82.9 (C-4), 72.7, 72.3 (C-2, C3), 70.0 (C-5), 53.3 (C-7; $CHNH_3$), 39.5 (C-6), 39.2 (C-11; CH_2NH_3), 30.9, 26.6, 21.8 (C-8, C-9, C-10; CH_2). For $C_{72}H_{138}N_{18}O_{30}$ (M_w = 1735), MS (MALDI-TOF/TOF): 1736.0 uma $[M + H^+]$.

Polymers. PLK_6 and PLK_{190}—poly(L-lysine) with degree of polymerization of 6 and 190, respectively—were purchased from Sigma Aldrich and Bachem (Bubendorf, Switzerland), respectively. $K_{20}H_{20}$ was a poly(L-lysine) with degree of polymerization of 20 (NeoMPS SA, Strasbourg, France) in which all the ε-amino functions of the lysyl residues were substituted with histidine residues as described.[19]

Cells and Cell Culture. Human embryonic kidney 293T7 cells were grown at 37 °C in a humidified atmosphere containing 5% CO_2 in MEM medium containing 10% heat inactivated fetal bovine serum (PAA Laboratories, Les Mureaux, France), 2 mM L-glutamine (Fischer Bioblock, Illkirch, France), 100 U/mL penicillin (Fischer Bioblock), 100 U/mL streptomycin (Fischer Bioblock), and Geneticin (400 μg/mL).[20] Cells were mycoplasma-free as evidenced by MycoAlert Mycoplasma Detection Kit (Lonza, Levallois Perret, France).

Plasmids. pTG11033 (pCMV-Luc; 9514 bp) (kindly given by Transgene S.A., Strasbourg, France) was a plasmid DNA encoding the *firefly* luciferase gene under the control of the

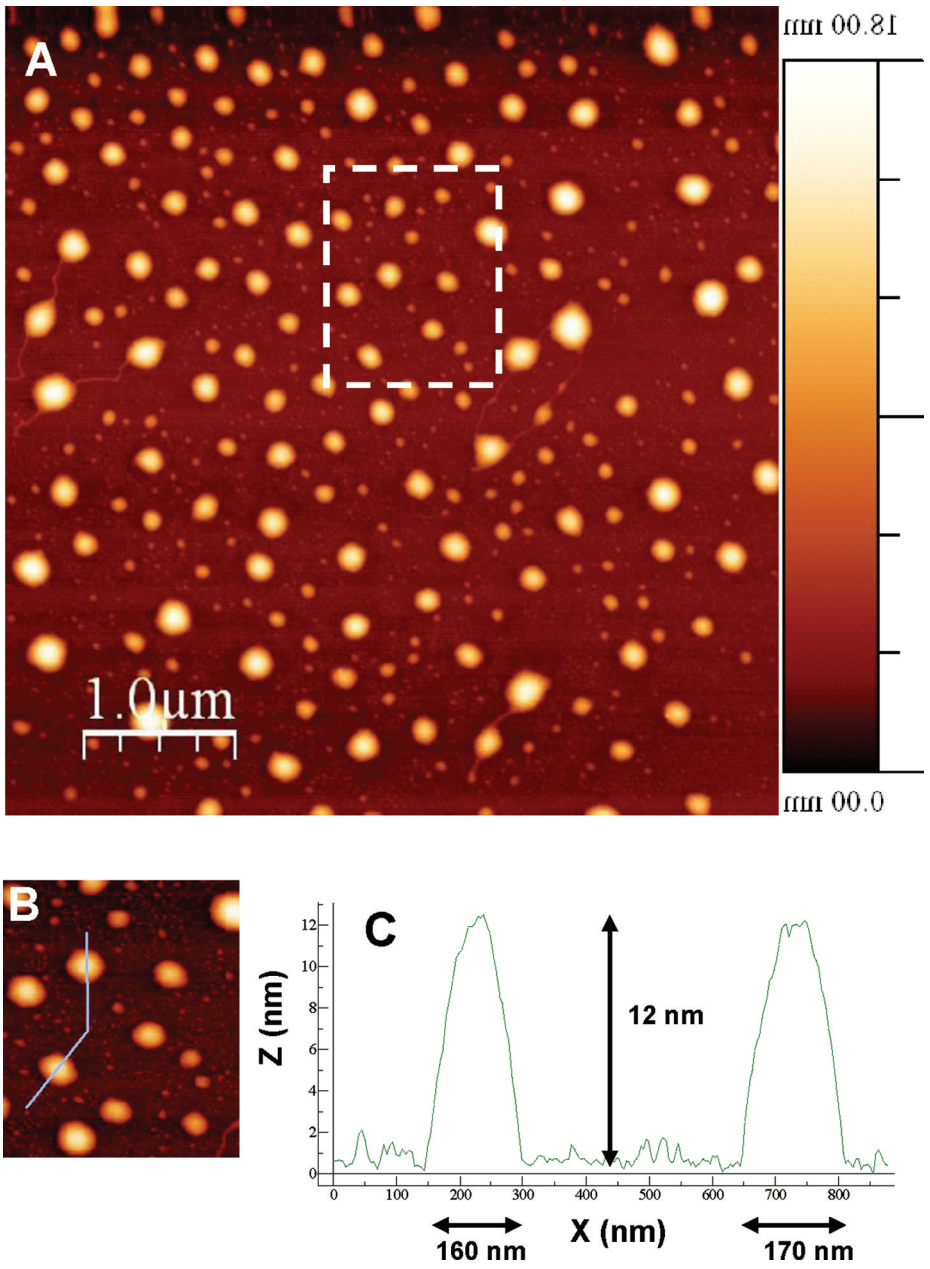

Figure 3. AFM morphology of His-α-CD/pDNA complexes (N/P of 4.2). (A) 2D topography: tapping mode in air; scan size: 5 μm, scan rate: 0.603 Hz, I. Gain: 0.4, P. Gain: 0.5, Amp. Set.: 1.1 V (−0.067 V/ASAE), Drive Amp.: 25 mV, Z Limit: 850 nm. Scale intensity. Bar next to images represents the *Z* scale in nm. (B) image in the square. (C) AFM profile of His-α-CD/pDNA complexes along the line in image in (B) where *Z* is the height and *X* the diameter.

human cytomegalovirus promoter. Supercoiled plasmid DNA was isolated by a standard alkaline lysis method, and purification was carried out with the QIAGEN Mega Kit (QIAGEN, Courtaboeuf, France).

Dye Exclusion Experiments. Aliquots of solution containing cationic derivatives were sequentially added to pDNA (2.5 μg) in 650 μL of 10 mM Hepes buffer, pH 7.4, in the presence of ethidium bromide (2 μM). The fluorescence intensity was measured (λ_{ex} = 530 nm; λ_{em} = 580 nm) after each addition of samples and the fraction of dye exclusion was calculated from the fluorescence intensity measured in the absence and in the presence of cationic derivatives.

Measurements of Size and ζ Potentials. CDplexes were prepared by adding 40 μg of His-α-CD or Lys-α-CD in 60 μL of 10 mM Hepes buffer, pH 7.4, to 10 μg pDNA in 140 μL of 10 mM Hepes buffer, pH 7.4. The solution was mixed by up−down pipetting, vortexed for 4 s, and allowed to stand for 30 min at 20 °C. Then, CDplexes were diluted to 1.4 mL in 10 mM Hepes buffer, pH 7.4. Their size and their ζ potential were measured with ZetaSizer 3000 (Malvern Instruments, Orsay, France). The size was measured by quasi-elastic laser light scattering (QELS) with a sample refractive index of 1.59 and a viscosity of 0.89. The system was calibrated with the 200 ± 5 nm polystyrene polymers (Duke Scientific Corps, Palo Alto, CA). The diameter of CDplexes was calculated in the automatic mode. Their ζ potential was measured by electrophoretic mobility. The following parameters were set up: viscosity, 0.891 cP; dielectric constant, 79; temperature, 25 °C;

dx.doi.org/10.1021/bc200167p | *Bioconjugate Chem.* 2011, 22, 2404−2414

F(Ka), 1.50 (Smoluchowsky); maximum voltage of the current, 15 V. The system was calibrated with DTS 5050 standard from Malvern. Measurements were done ten times with the zero-field correction. The ζ potential was calculated with the Smoluchowsky approximation.

Atomic Force Microscopy. Two microliter aliquots of His-α-CD/pDNA complexes at a mass ratio of 4:1 prepared in 10 mM hepes buffer were adsorbed for 5 min on freshly cleaved muscovite mica. The surface was rinsed thoroughly with ultrapure water and dried for 2 h under vacuum-drying. AFM imaging was performed in tapping mode with Tap300A1-G tip (Budget Sensors, Combo, US) at a scanning speed of 0.603 Hz with an AFM Veeco Dimension 3100 (Veeco, Santa Barbara, CA) using high frequency (300 kHz) and Tap300Al-G silicon probe with tip radius <10 nm (Budget Sensors). Images were treated using the *WSxM 5.0* software.[21]

Transfections. Two days prior to transfection, cells were seeded at 1×10^5 cells per 2 cm^2 in culture medium (1 mL) in a 24-well plate. At the time of the experiment, cell cultures were 80% confluent. CDplexes were prepared by adding 30 μg of His-α-CD or Lys-α-CD in 45 μL of 10 mM Hepes buffer, pH 7.4, to 7.5 μg pDNA in 105 μL of 10 mM Hepes buffer, pH 7.4. The solution was mixed by up−down pipetting, vortexed for 4 s, and allowed to stand for 30 min at 20 °C. It was adjusted to 1.5 mL with culture medium supplemented with 10% FBS before transfection. The medium was removed, the CDplex solution (0.5 mL, 2.5 μg pDNA) was added in each well, and cells were incubated for 4 h at 37 °C. Then, the medium was removed, and cells were cultured 48 h at 37 °C in complete culture medium. Luciferase activity was measured using a Lumat LB9507 luminometer (Lumat LB9507, Berthold, Wildbach, Germany), and the luciferase activity (Relative Light units, RLU) was normalized to RLU per milligram extracted protein.[22]

NMR Experiments. NMR experiments were carried out in D_2O using an Avance 300 MHz Bruker instrument, except for the rotating frame Overhauser effect spectroscopy (ROESY) and heteronuclear 2D experiments which were realized using an Avance 600 MHz Bruker instrument. The temperature calibration of the 300 MHz spectrometer was performed with a sample of 100% CH_3OH in the temperature range between 298 and 313 K.

For the diffusion-ordered spectroscopy (DOSY) experiments, the maximum field gradient strength was calibrated using a homemade Plexiglas phantom (8 mm ±0.01 length and a width equal to the inner diameter of the NMR tube) inserted in a H_2O-filled NMR tube and using the pulse program *calibgp*.[23] Some "negative" projection images of the phantom as a function of applied field gradient strength is given (Supporting Information Figure S2). The linear plot of the obtained gradient strengths against the gradient strength setting (GPZ1) used gave a maximum field gradient strength equal to 56.8 G/cm. The accuracy of the calibrations was checked by measuring the self-diffusion coefficient of a mixture H_2O/D_2O (10%/90% in moles) at 25 °C.[24] The DOSY experiments were carried out using the stegp1s pulse sequence with a linear gradient of 16 steps between 2% and 95%. Before each diffusion experiment, the proton relaxation times were determined in order to correctly set the D1 parameter of the DOSY sequence, and the length of the gradient δ and the diffusion time Δ were optimized for each analyzed product.

RESULTS AND DISCUSSION

Synthesis of α-CD Derivatives. Hexakis(6-deoxy-6-amino)cyclomaltohexaose was synthesized according to previous reported procedures. Then, the coupling between protected amino acid and hexakis(6-deoxy-6-amino)-cyclomaltohexaose were conducted following two synthetic pathways in order to reach a good yield of each product (Scheme 1). Deprotection of the amine functions of the grafted amino groups were then performed to obtain the expected products. ^{1}H NMR (SI Figures S3 and S4) and ^{13}C NMR (SI Figure S5 and S6) spectra show that His-α-CD and Lys-α-CD were synthesized with good purity. MS (MALDI-TOF/TOF) spectrum of the histidinylated conjugate show peaks at 1795.8 and 1827.8 uma (respectively, Li^+ and K^+ adducts) confirming the presence of α-CD substituted by 6 histidyl residues (SI Figures S7). MS (MALDI-TOF/TOF) spectrum of the lysylate conjugate indicated a molecular weight of 1736 uma corresponding to α-CD substituted with 6 lysyl residues (SI Figures S8). Undersubstitution of the CD was detected by mass spectroscopy as witnessed by the presence of a peak at 1608.9 uma, which corresponds to modified cyclodextrin with one glucopyranose unit having an hydroxyl function at the 6 position (SI Figure S8). This compound was found to form a complex with HOBt-TFA salt, demonstrated by a peak at 1880.1 uma, at a concentration not detectable by NMR.

Interaction of Polyamino α-CD Derivatives with DNA. The ability of each polyamino α-CD to condense a plasmid DNA was evaluated by fluorescence dye exclusion using ethidium bromide. This nonfluorescent molecule becomes fluorescent once intercalated between the base pairs of the plasmid DNA. Conversely, the fluorescence intensity drops due to dye exclusion when DNA condensation occurs in the presence of polycationic molecules. As shown in Figure 1, the dye exclusion depended on the polyamino α-CD types. The fluorescence intensity decreased rapidly when the amount of His-α-CD increased, indicating a strong condensation of the plasmid DNA. The maximum of the dye exclusion reached 80% in the presence of 7.5 μg (4.2 nmol) His-α-CD corresponding to a N/P charge ratio of 4.2. N/P was the charge ratio between the number of positive charges of the polyamino α-CD derivatives and the negative charges of the pDNA phosphate. All the pDNA phosphate functions are negatively charged and the 12 amino groups of Lys-α-CD are positively charged at pH 7.4. On the basis of our previous results on histidylated polylysine, we have hypothesized that His-α-CD contained 8 positive charges at pH 7.4. We have indeed reported that the protonation of the imidazole groups in histidylated polylysine occurs at a 1.1 pH unit higher (6.9) than that of histidine, meaning that 2 of the 6 imidazole rings are protonated at pH 7.4.[25] Surprisingly, no significant dye exclusion and no DNA condensation were observed in the presence of NH_2-α-CD. The fluorescence intensity decreased much more in the presence of Lys-α-CD than in the presence of NH_2-α-CD. The maximum of the dye exclusion reached 50% in the presence of 17 μg (120 nmol) Lys-α-CD at N/P of 15. While Lys-α-CD contained more positive charges than His-α-CD, DNA condensation with Lys-α-CD was lower than with His-α-CD. The formation of DNA complexes with the polyamino α-CD derivatives was monitored by agarose gel electrophoresis (Figure 2). The gel retardation experiments indicated that no migration of 1 μg pDNA was observed from 1 μg His-α-CD and 2 μg Lys-α-CD. Compared to pDNA/Lys-α-CD, the lower

level of BET staining of pDNA with His-α-CD from a 1/1 weight ratio evidenced a better DNA condensation that was in line with dye exclusion experiments. In these weight ratios, the migration of pDNA was observed with α-CD-NH_2 confirming the absence of pDNA condensation (not shown).

Physicochemical Parameters of DNA/Polyamino α-CD Derivatives Complexes (CDplexes). The size and the ζ potential of CDplexes were measured at their optimal DNA/CD ratio. Dynamic light scattering measurements of His-α-CDplexes at N/P of 4.2 indicated that their diameter was close to 225 ± 45 nm with a polydispersity index (PDI) of 0.31 indicative of a relative homogeneity of the size distribution. These CDplexes were slightly positive (ζ potential = 7 ± 5 mV). In contrast, the size of Lys-α-CDplexes at same N/P was close to 640 ± 90 nm (PDI of 0.64) and the ζ potential was −1 ± 3 mV. This result confirmed the higher DNA condensation capacity of His-α-CD. The lower DNA condensation capacity of Lys-α-CD formed larger and less homogeneous CDplexes. His-α-CDplexes were cast on mica and observed by AFM. All the pDNA was complexed with His-α-CD and formed globular particles (Figure 3A,B). On the basis of the AFM profiles, His-α-CDplexes demonstrated the average diameter and height of 170 and 12 nm, respectively (Figure 3C). Compared to DLS, the CDplexes dimension was slightly smaller with AFM because AFM provides measurement of a single particle, while DLS gives the mean value for the non-monodispersed solution of particles.[26]

Transfection Efficiency. The ability of these CDplexes to transfect mammalian cells was examined using HEK293-T7 cells and pCMVLuc, a plasmid encoding the luciferase gene. The cells were incubated for 4 h with CDplexes containing 2.5 μg pDNA. Figure 4 shows that the luciferase activity in cells

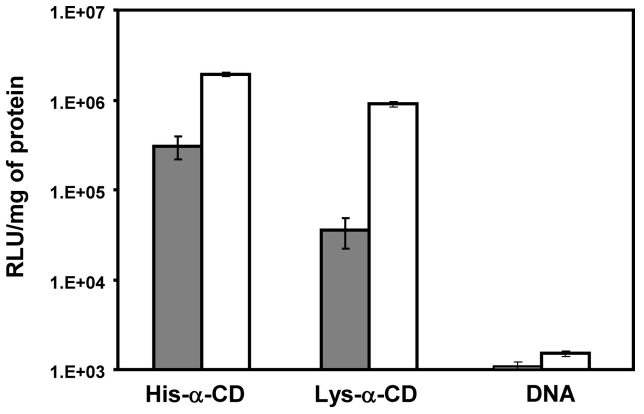

Figure 4. Transfection of HEK293-T7 cells with CDplexes. Cells were transfected with pCMVLuc (2.5 μg) free or complexed with His-α-CD or Lys-α-CD at N/P of 5.3 and 8.5, respectively. Transfection was carried out in the absence (gray bars) or the presence (white bars) of 100 μM chloroquine. The luciferase activity expressed as relative light units per mg protein (RLU/mg of protein) was measured upon 48 h of culture. The values shown are averages of three independent experiments.

transfected with His-α-CDplexes (3×10^5 RLU/mg of protein) was 8-fold higher than that obtained Lys-α-CDplexes. When the transfection was carried out in the presence of chloroquine—a lysosomotropic reagent that favors destabilization of acid vesicles [27]—the luciferase activity of His-α-CDplexes and Lys-α-CDplexes increased 6 and 25 times, respectively. The enhancement was lower with His-α-CD compared to Lys-α-CD, because His-α-CD contains acid-protonable imidazole groups that induce a proton sponge effect inside endosomes which favors the delivery of pDNA into the cytosol in the absence of chloroquine. Here, the protonation behavior of the imidazole groups in His-α-CDplexes is expected to be as in polyplexes made with histidylated polylysine (His-pLK). We have indeed reported that the ζ potential of His-pLK polyplexes increased 8 times when the pH decreased from 7.5 to 5.0 indicating that the protonation of the imidazole groups in His-pLK occurs in polyplexes.[25] The transfection efficiency of His-α-CD was about 3 orders of magnitude lower than that of lPEI (6×10^8 RLU/mg proteins), the gold standard cationic polymer. Nevertheless, the transfection efficiency of His-α-CD was as high as that of HeLa and H9c2 cells with pDNA complexed with a β-cyclodextrin substituted with seven tetraethylenpentamine residues.[28] It was close to the transfection of HEK293 cells with pCMV-Luc complexed with a *per* ethylenimine α-CD (2×10^6 RLU/mg of protein) that contained also protonable amines.[2] Of note, DNA complexed with *per* oligoethylenimine α-CD became very efficient (1×10^9 RLU/mg proteins) when the number of ethylenimine repeat units reached 4.[8]

Comparative DNA Condensation Capacity of His-α-CD and Poly(L-lysines). The unexpected DNA condensation capacity of His-α-CD prompted us to compare this ability with that of other cationic polymers such as poly(L-lysine) by using fluorescence dye exclusion. Surprisingly, DNA condensation with His-α-CD (8 NH_2 functions per CD molecule) was close to that observed with PLK_{190} (190 NH_2 functions per polymer molecule) (Figure 5). The maximum of the dye exclusion

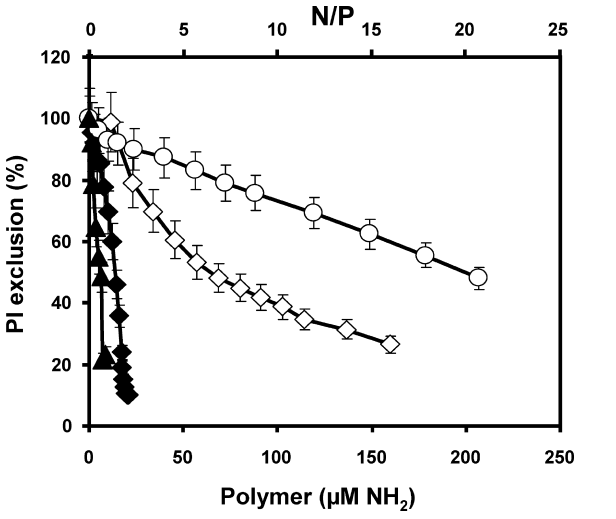

Figure 5. Interaction of polymers with DNA. Aliquots of solution containing polymers were sequentially added to pDNA (2.5 μg) in 650 μL of 10 mM Hepes buffer, pH 7.4, in the presence of ethidium bromide (2 μM). The fluorescence intensity was measured (λ_{ex} = 530 nm; λ_{em} = 580 nm) after each addition of sample and the fraction of dye exclusion was calculated from the fluorescence intensity measured in the absence and in the presence of polymers. N/P corresponds to the ratio between the number of positive charges of polymers and that of the negative charges of the pDNA phosphate. His-α-CD (▲); PLK_{190} (◆); PLK_6 (◇); $K_{20}H_{20}$ (○).

reached 90% in the presence of 0.11 μM (i.e., 21 μM NH_2) PLK_{190} at N/P of 2. The DNA condensation capacity of His-α-CD was higher than with PLK_6 containing 6 NH_2 functions per

dx.doi.org/10.1021/bc200167p | Bioconjugate Chem. 2011, 22, 2404–2414

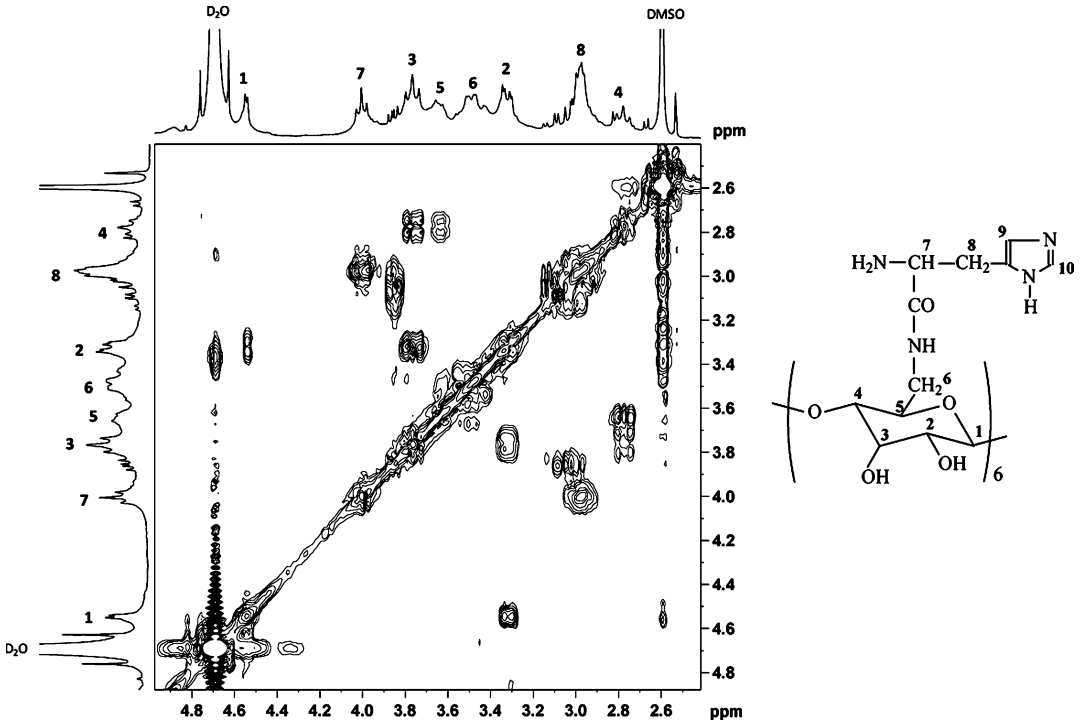

Figure 6. COSY NMR experiment of His-α-CD.

polymer molecule (Figure 5). Surprisingly, the DNA condensation was much higher with His-α-CD than with $K_{20}H_{20}$ (Figure 5). This latter polymer was a poly(L-lysine) of 20 lysyl residues that were substituted with a histidine residue linked on their ε-amino group. On the basis of the number of positive charges, one would be expected that DNA condensation will be stronger with $K_{20}H_{20}$ than with His-α-CD. Note that the DNA condensation with $K_{20}H_{20}$ was also lower than with PLK_6. Therefore, the DNA condensation capacity of His-α-CD did not involve only interaction of the positive charges of the α-CD derivative with the phosphate groups of the nucleic acid, but suggested the formation of a supramolecular structure allowing cooperative interaction with DNA involving CD and histidine. Indeed, it is known that the imidazole group can form an inclusion complex with the hydrophobic cavity of cyclodextrin.[29] Binding constants of imidazole to α-cyclodextrin are approximately 6 times higher than those for β-cyclodextrin as measured by microcalorimetric technique. Therefore, we have examined by NMR investigation the possible formation of supramolecular structures from His-α-CD molecules which could explain the strong interaction with pDNA.

Characterization of Supramolecular Association by NMR. *CD Derivatives ROESY NMR Experiments.* First, 1D and 2D NMR of His-α-CD were performed to confirm the structure of the product. On the basis of the ^{1}H NMR spectra of the initial reactants and on the correlation spectroscopy (COSY) NMR spectrum, all the peaks of the His-α-CD ^{1}H spectrum were assigned (Figure 6). It was observed that integration of the peak at 7.75 ppm of the proton borne by the carbon between the two nitrogen atoms decreased with time until complete exchange with deuterium. This fact was also observed for each imidazole derivative. The heteronuclear single quantum correlation (HSQC) experiment of His-α-CD was used to identify each carbon of the product (SI Figure S9).

To examine the possible formation of supramolecular structures from His-α-CD molecules, a 2D ROESY NMR experiment was carried out to determine which protons were close to each other in space even if they were not bonded. The spectrum in Figure 7 shows that the CD proton H5, which is located inside the CD cavity, is correlated to the proton H9 of the imidazole group *via* an intense negative cross-peak, whereas there is no cross-peak between the proton H5 and the proton H10 belonging to the imidazole group. In the same way, we observe a negative cross-peak between the protons H3 and H10 and no correlation between H3 and H9. This result demonstrates that an inclusion complex occurs through the CD primary side. Discrimination between intra- (Figure 8b) and intermolecular (Figure 8c) interaction between the CD cavity and the imidazole moieties requires more investigation. When the same experiments were performed with Lys-α-CD, the 2D ROESY NMR spectrum showed no negative cross-peak between the proton H5 of the CD and the methylene groups of the lysine (peaks 8, 9, and 10), indicating the absence of inclusion between lysyl residue and the hydrophobic cavity of CD (SI Figure S10, Figure 9).

CD Derivatives DOSY NMR Experiments. Diffusion-ordered spectroscopy (DOSY) experiments were attempted to determine whether His-α-CD allowed supramolecular assemblies or not. DOSY NMR which is based on a pulse-field gradient spin−echo NMR experiment, in which components experience diffusion, provides relevant information for the study of mixtures or for the structure characterization of polymers (see Supporting Information).[30,31] On the basis of the scheme in Figure 8c, His-α-CD supramolecular species would be dimers or higher molecular weight species. Thus, a decrease of the diffusion coefficients would be correlated to the increase of the molecular weight of the molecules. First, the diffusion coefficients of D_2O, L-histidine, and α-CD in an equimolar mixture of α-CD and L-histidine were, respectively, found equal

dx.doi.org/10.1021/bc200167p | *Bioconjugate Chem.* 2011, 22, 2404−2414

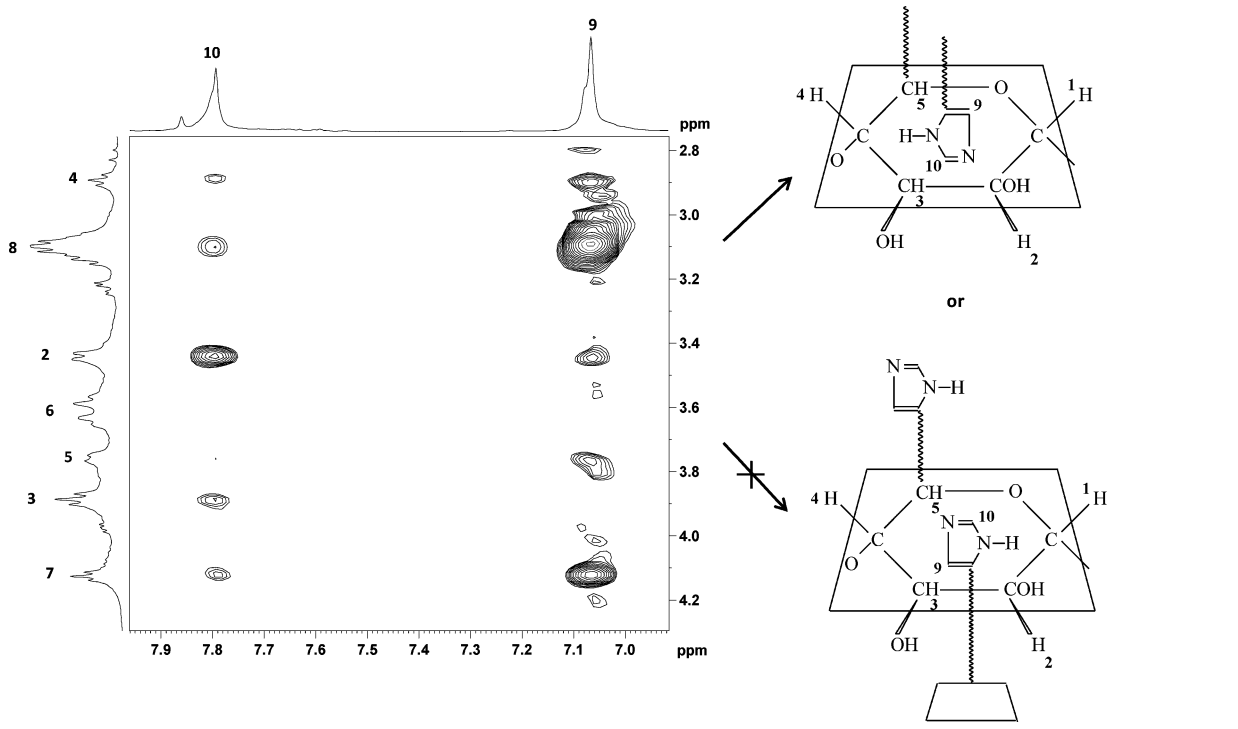

Figure 7. Zoomed ROESY NMR experiment of His-α-CD in D_2O.

to 1.86×10^{-9} $m^2.s^{-1}$, 5.92×10^{-10} $m^2.s^{-1}$, and 2.82×10^{-10} $m^2.s^{-1}$ (SI Figures S11 and S12; Table 1). Then, the diffusion coefficient of α-CD alone (2.78×10^{-10} $m^2.s^{-1}$) or in an equimolar mixture with methyl-L-histidine (2.83×10^{-10} $m^2.s^{-1}$) were determined (Table 1). The DOSY treatment of His-α-CD alone gave a diffusion coefficient of 1.93×10^{-10} $m^2.s^{-1}$ from the peak at ~7.0 ppm or 2.21×10^{-10} $m^2.s^{-1}$ taking into account the broad peak located between 2.8 ppm and 4.3 ppm (protons from the CD and histidine group) (SI Figure S13; Table 1). These close values confirm that the imidazole group was linked to α-cyclodextrin. The DOSY treatment of Lys-α-CD gave 1.85×10^{-10} $m^2.s^{-1}$ from the anomeric peak, 1.83×10^{-10} $m^2.s^{-1}$ from the broad peak between 4.2 and 3.1 ppm, 1.75×10^{-10} $m^2.s^{-1}$ from the peak at 2.9 ppm, 1.87×10^{-10} $m^2.s^{-1}$ from the peak at 1.9 ppm, 1.78×10^{-10} $m^2.s^{-1}$ from the peak at 1.6 ppm, and 1.86×10^{-10} $m^2.s^{-1}$ from the peak at 1.35 ppm (SI Figure S14). These values were very close, giving an average diffusion coefficient of 1.83×10^{-10} $m^2.s^{-1}$ (Table 1).

Overall, these experiments show that the diffusion rates of the solvent molecules are almost the same whatever the considered DOSY and corresponds to the highest values compared to the investigated molecules. When α-CD is substituted with α-amino acids, the diffusion coefficient is lower than the initial α-CD in agreement with its higher hydrodynamic volume. The comparison of the two grafted α-CD (having a similar molar mass) shows that the diffusion coefficient of His-α-CD is slightly higher than that of Lys-α-CD, explained by the higher hydrodynamic volume of the protonated Lys-α-CD compared to that of His-α-CD. The diffusion coefficient measurements of His-α-CD were confirmed by increasing the attenuation, i.e., the values of Δ and δ (run 5, Table 1). The signal-to-noise ratio decrease was compensated by a higher number of scans (run 6, Table 1), and no variation of the diffusion coefficient was noticed (runs 4, 5 and 6, Table 1). Taking in account the ROESY experiment showing the interaction between the imidazole ring and the hydrophobic cavity of the α-CD, and the diffusion values, it appears that only intramolecular interactions occur between His-α-CD molecules under NMR conditions. Compared with transfection experiments, NMR experiments with His-α-CD were performed at a much higher CD concentration (~100 times higher), and no large diffusive species was detected, suggesting that the supramolecular association of His-α-CD was not favored under any NMR conditions, i.e., without plasmid added to the CD derivatives. During His-α-CDplex formation, interaction between amino groups of His-α-CD and DNA phosphate moieties might provide a scaffold for a template association of His-α-CD via inclusion complexes between CD and the histidine moieties (Figure 8c). This effect can be compared to the spontaneous polymerization by disulfide bond when sulfhydryl cross-linking peptides or polymers were bound to pDNA leading to stable DNA condensates.[32−34]

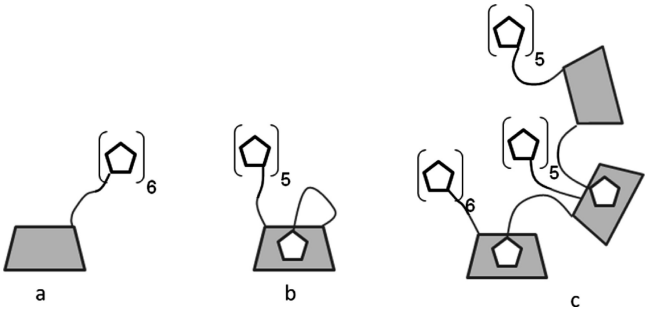

Figure 8. Schematic representation of the various forms of CD derivatives.

dx.doi.org/10.1021/bc200167p | Bioconjugate Chem. 2011, 22, 2404−2414

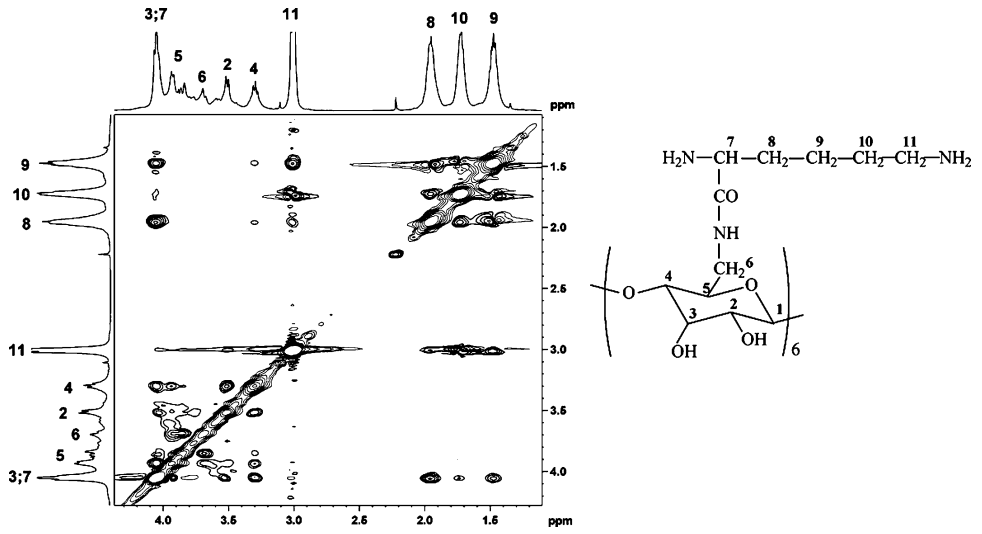

Figure 9. ROESY NMR experiment of Lys-α-CD in D_2O.

Table 1. DOSY NMR Experiments: Determination of the Diffusion Coefficients (D) of Different Samples[a]

		D ($m^2.s^{-1}$)		
run	signal used for the D determination	peak at 7 ppm	H_1	CD broad
1	α-CD		2.78×10^{-10}	2.70×10^{-10}
2	mixture (1/1) α-CD/histidine	5.92×10^{-10}	2.82×10^{-10}	
3	mixture (1/1) α-CD/Me-Lhistidine	5.32×10^{-10}	2.83×10^{-10}	
4	His-α-CD	1.93×10^{-10}		2.21×10^{-10}
5	His-α-CD	2.00×10^{-10}		2.11×10^{-10}
6	His-α-CD	2.05×10^{-10}		2.10×10^{-10}
7	Lys-α-CD		1.85×10^{-10}	1.83×10^{-10}

[a] $M_{\alpha CD}$ = 972 g/mol; $M_{histidine}$ = 155 g/mol; $M_{Me\text{-}Lhistidine}$ = 169 g/mol; $M_{His\text{-}\alpha\text{-}CD}$ = 1789 g/mol; $M_{Lys\text{-}\alpha\text{-}CD}$ = 1735 g/mol. Runs 1,2,34: Δ = 200 ms and δ = 4.5 ms; runs 5 and 6: Δ = 300 ms and δ = 6 ms. Note that no calculation was conducted from the peak at 7.7 ppm because it disappeared with time, and from the anomeric CD proton which overlapped with the solvent peak for His-α-CD.

CONCLUSION

In the present work, we demonstrated that His-α-CD can condense a plasmid DNA allowing the formation of CDplexes that transfect cells. At the same time, we found that the DNA condensation capacity of His-α-CD is unexpectedly higher than that obtained with the lysyl-α-CD counterpart. NMR studies demonstrated that the formation of an inclusion complex between histidine and the hydrophobic cavity of CD occurs and only intramolecular interaction occurs between His-α-CD molecules in the absence of DNA. These results suggest that intermolecular interactions between imidazole and His-α-CD cavity can take place to form supramolecular assemblies in the presence of a DNA scaffold increasing the DNA condensation.

ASSOCIATED CONTENT

Supporting Information

Experimental protocol. His-α-CD DOSY NMR experiments. Images projection of the phantom with increasing gradient strength (only images obtained with 5% to 50% of the maximum gradient strength are shown; a residual signal is observed due to water in the inside screw thread for ease of phantom handling). ^1H NMR of hexakis(6-deoxy-6-histidinyl)cyclomaltohexaose (His-α-CD). ^1H NMR of hexakis(6-deoxy-6-lysinyl)-cyclomaltohexaose (Lys-α-CD). ^{13}C NMR of hexakis(6-deoxy-6-histidinyl)cyclomaltohexaose (His-α-CD). ^{13}C NMR of hexakis(6-deoxy-6-lysinyl)cyclomaltohexaose (Lys-α-CD). MS (MALDI-TOF/TOF) spectrum of hexakis(6-deoxy-6-histidinyl)-cyclomaltohexaose (His-α-CD). MS (MALDI-TOF/TOF) spectrum of hexakis(6-deoxy-6-lysinyl)cyclomaltohexaose (Lys-α-CD). HSQC experiment of His-α-CD in D_2O (experiment with water suppression, which explains the reason the D_2O and anomeric proton signals did not appear). COSY experiment of Lys-α-CD in D_2O at 25.2 °C; [Lys-α-CD] = 9.3×10^{-3} mol/L. ^1H spectrum of a mixture (1/1) of αCD and L-histidine in D_2O at 25.2 °C; [αCD] = [L-histidine] = 21.6×10^{-3} mol/L. ln I versus $\gamma^2g^2\delta^2(\Delta-\delta/3)$ plot considering the anomeric proton at 4.97 ppm; [α-CD] = [L-histidine] = 21.6×10^{-3} mol/L in D_2O; 25.2 °C. ln I versus $\gamma^2g^2\delta^2(\Delta-\delta/3)$ plot considering the peaks resonated between 4.3 and 2.8 ppm. [His-α-CD] = 9.0×10^{-3} mol/L in D_2O; 25.2 °C; Δ = 200 ms; δ = 4.5 ms. ln I versus $\gamma^2g^2\delta^2(\Delta-\delta/3)$ plot considering the peaks resonated between 4.2 and 3.1 ppm; [Lys-α-CD] = 9.3×10^{-3} mol/L in D_2O; 25.2 °C. This material is available free of charge via the Internet at http://pubs.acs.org.

AUTHOR INFORMATION

Corresponding Author

*Phone: +33 2 38 25 55 65; E-mail: patrick.midoux@cnrs-orleans.fr.

Author Contributions

[#]Both investigators contributed equally and should be considered as senior authors.

■ ACKNOWLEDGMENTS

We warmly thank Cristine Gonçalves, Loic Lebègue, and Marie-Jeanne Clement for their excellent technical assistance. We are grateful to Fréderic Foucher for AFM analyses. We thank Guillaume Gaban and the Mass Spectroscopy platform of CBM for mass spectroscopy analyses. This work was supported by grants from Association Française contre les Myopathies (AFM) and Vaincre La Mucoviscidose (VLM).

■ REFERENCES

(1) Ortiz Mellet, C., Garcia Fernandez, J. M., and Benito, J. M. (2010) Cyclodextrin-based gene delivery systems. *Chem. Soc. Rev. 40*, 1586−1608.

(2) Yang, C., Li, H., Goh, S. H., and Li, J. (2007) Cationic star polymers consisting of alpha-cyclodextrin core and oligoethylenimine arms as nonviral gene delivery vectors. *Biomaterials 28*, 3245−3254.

(3) Srinivasachari, S., Fichter, K. M., and Reineke, T. M. (2008) Polycationic beta-cyclodextrin "click clusters": monodisperse and versatile scaffolds for nucleic acid delivery. *J. Am. Chem. Soc. 130*, 4618−4627.

(4) Diaz-Moscoso, A., Balbuena, P., Gomez-Garcia, M., Ortiz Mellet, C., Benito, J. M., Le Gourrierec, L., Di Giorgio, C., Vierling, P., Mazzaglia, A., Micali, N., Defaye, J., and Garcia Fernandez, J. M. (2008) Rational design of cationic cyclooligosaccharides as efficient gene delivery systems. *Chem. Commun. (Camb.)*, 2001−2003.

(5) Diaz-Moscoso, A., Le Gourrierec, L., Gomez-Garcia, M., Benito, J. M., Balbuena, P., Ortega-Caballero, F., Guilloteau, N., Di Giorgio, C., Vierling, P., Defaye, J., Ortiz Mellet, C., and Garcia Fernandez, J. M. (2009) Polycationic amphiphilic cyclodextrins for gene delivery: synthesis and effect of structural modifications on plasmid DNA complex stability, cytotoxicity, and gene expression. *Chemistry 15*, 12871−12888.

(6) Ortega-Caballero, F., Mellet, C. O., Le Gourrierec, L., Guilloteau, N., Di Giorgio, C., Vierling, P., Defaye, J., and Garcia Fernandez, J. M. (2008) Tailoring beta-cyclodextrin for DNA complexation and delivery by homogeneous functionalization at the secondary face. *Org. Lett. 10*, 5143−5146.

(7) Peres, B., Richardeau, N., Jarroux, N., Guegan, P., and Auvray, L. (2008) Two independent ways of preparing hypercharged hydrolyzable polyaminorotaxane. *Biomacromolecules 9*, 2007−2013.

(8) Yang, C., Wang, X., Li, H., Goh, S. H., and Li, J. (2007) Synthesis and characterization of polyrotaxanes consisting of cationic alpha-cyclodextrins threaded on poly[(ethylene oxide)-ran-(propylene oxide)] as gene carriers. *Biomacromolecules 8*, 3365−3374.

(9) Choi, H. S., Ooya, T., and Yui, N. (2006) One-pot synthesis of a polyrotaxane via selective threading of a PEI-b-PEG-b-PEI copolymer. *Macromol. Biosci. 6*, 420−424.

(10) Wang, C. Y., and Huang, L. (1984) Polyhistidine mediates an acid-dependent fusion of negatively charged liposomes. *Biochemistry 23*, 4409−4416.

(11) Uster, P. S., and Deamer, D. W. (1985) pH-dependent fusion of liposomes using titratable polycations. *Biochemistry 24*, 1−8.

(12) Midoux, P., and Monsigny, M. (1999) Efficient gene transfer by histidylated polylysine/pDNA complexes. *Bioconjug. Chem. 10*, 406−411.

(13) Midoux, P., Pichon, C., Yaouanc, J. J., and Jaffres, P. A. (2009) Chemical vectors for gene delivery: a current review on polymers, peptides and lipids containing histidine or imidazole as nucleic acids carriers. *Br. J. Pharmacol. 157*, 166−178.

(14) Rodal, S. K., Skretting, G., Garred, O., Vilhardt, F., van Deurs, B., and Sandvig, K. (1999) Extraction of cholesterol with methyl-beta-cyclodextrin perturbs formation of clathrin-coated endocytic vesicles. *Mol. Biol. Cell 10*, 961−974.

(15) Kilsdonk, E. P., Yancey, P. G., Stoudt, G. W., Bangerter, F. W., Johnson, W. J., Phillips, M. C., and Rothblat, G. H. (1995) Cellular cholesterol efflux mediated by cyclodextrins. *J. Biol. Chem. 270*, 17250−17256.

(16) Ohtani, Y., Irie, T., Uekama, K., Fukunaga, K., and Pitha, J. (1989) Differential effects of alpha-, beta- and gamma-cyclodextrins on human erythrocytes. *Eur. J. Biochem. 186*, 17−22.

(17) Benkhaled, A., Cheradame, H., Fichet, O., Teyssié, D., and Guégan, P. (2008) Synthesis and characterization of amphiphilic per-(6-thio-2,3-trimethylsilyl) cyclodextrin: application to langmuir film formation. *Polym. Carbohydr. 73*, 482−489.

(18) Guillo, F., Hamelin, B., Julien, L., Canceill, J., Lehn, J.-M., De Robertis, L., and Driguez, H. (1995) Synthesis of symmetrical cyclodextrin derivatives bearing multiple charges. *Bull. Soc. Chim. Fr. 132*, 857−866.

(19) Pichon, C., Roufai, M. B., Monsigny, M., and Midoux, P. (2000) Histidylated oligolysines increase the transmembrane passage and the biological activity of antisense oligonucleotides. *Nucleic Acids Res. 28*, 504−512.

(20) Brisson, M., He, Y., Li, S., Yang, J. P., and Huang, L. (1999) A novel T7 RNA polymerase autogene for efficient cytoplasmic expression of target genes. *Gene Ther. 6*, 263−270.

(21) Horcas, I., Fernandez, R., Gomez-Rodriguez, J. M., Colchero, J., Gomez-Herrero, J., and Baro, A. M. (2007) WSXM: a software for scanning probe microscopy and a tool for nanotechnology. *Rev. Sci. Instrum. 78*, 013705.

(22) Midoux, P., Mendes, C., Legrand, A., Raimond, J., Mayer, R., Monsigny, M., and Roche, A. C. (1993) Specific gene transfer mediated by lactosylated poly-L-lysine into hepatoma cells. *Nucleic Acids Res. 21*, 871−888.

(23) Seedhouse, S. J., and Hoffman, M. M. (2008) Magnetic field gradient calibration as an experiment to illustrate magnetic resonance imaging. *J. Chem. Educ. 85*, 836−838.

(24) Holz, M., and Weingärtner, H. (1991) Calibration in accurate spin-echo self-diffusion measurements using 1H and less-common nuclei. *J. Magn. Reson. 92*, 115−125.

(25) Bello Roufaï, M., and Midoux, P. (2001) Histidylated polylysine as DNA vector: Elevation of the imidazole protonation and reduced cellular uptake without change in the polyfection efficiency of serum stabilized negative polyplexes. *Bioconjugate Chem. 12*, 92−99.

(26) Hoo, C. M., Starostin, N., West, P., and Mecartney, M. L. (2008) A comparison of atomic force microscopy (AFM) and dynamic light scattering (DLS) methods to characterize nanoparticle size distributions. *J. Nanoparticle Res 10*, 89−96.

(27) Erbacher, P., Roche, A. C., Monsigny, M., and Midoux, P. (1996) Putative role of chloroquine in gene transfer into a human hepatoma cell line by DNA/lactosylated polylysine complexes. *Exp. Cell Res. 225*, 186−94.

(28) Srinivasachari, S., and Reineke, T. M. (2009) Versatile supramolecular pDNA vehicles via "click polymerization" of beta-cyclodextrin with oligoethyleneamines. *Biomaterials 30*, 928−938.

(29) Rekharsky, M. V., Nemykina, E. V., Eliseev, A. V., and Yatsimirsky, A. K. (1992) Thermodynamics of molecular recognition of nitrogen heterocycles: Part 1. Interation of imidazole and imidazolium cation with alpha cyclodextrin and beta cyclodextrin. *Thermochim. Acta 202*, 25−33.

(30) Williamson, R. T., Chapin, E. L., Carr, A. W., Gilbert, J. R., Graupner, P. R., Lewer, P., McKamey, P., Carney, J. R., and Gerwick, W. H. (2000) New diffusion-edited NMR experiments to expedite the duplication of known compounds from natural product mixtures. *Org. Lett. 2*, 289−292.

(31) Stessman, C. C., Ebel, R., Corvino, A. J., and Crews, P. (2002) Employing dereplication and gradient 1D NMR methods to rapidly characterize sponge-derived sesterterpenes. *J. Nat. Prod. 65*, 1183−1186.

(32) Park, Y., Kwok, K. Y., Boukarim, C., and Rice, K. G. (2002) Synthesis of sulfhydryl cross-linking poly(ethylene glycol)-peptides and glycopeptides as carriers for gene delivery. *Bioconjugate Chem. 13*, 232−239.

(33) Kwok, K. Y., Park, Y., Yang, Y., McKenzie, D. L., Liu, Y., and Rice, K. G. (2003) In vivo gene transfer using sulfhydryl cross-linked PEG-peptide/glycopeptide DNA co-condensates. *J. Pharm. Sci. 92*, 1174−1185.

(34) McKenzie, D. L., Smiley, E., Kwok, K. Y., and Rice, K. G. (2000) Low molecular weight disulfide cross-linking peptides as nonviral gene delivery carriers. *Bioconjugate Chem. 11*, 901−909.